RAPID COMMUNICATIONS IN MASS SPECTROMETRY, VOL. 10, 562–572 (1996)

In-situ Analysis of Lichen Pigments by Fourier Transform Laser Microprobe Mass Spectrometry with External Ion Source†

Wim Van Roy, Annick Mathey[1] and Luc Van Vaeck*

Department of Chemistry, University of Antwerp (U.I.A.), Universiteitsplein 1, B-2610 Wilrijk, Belgium
[1] Ministry of Agriculture (D.G.E.R.), 78, rue de Varenne, F-75349 Paris SP07, France

Several selected lichen samples are analysed by Fourier transform laser microprobe mass spectrometry with 5 μm resolution and with virtually no sample preparation. The application area can be increased to molecules with molecular weight higher than 500, because of the detection of post-laser generated ions. In most cases, enough information is available to allow, in combination with IR and NMR data, complete structural characterization of the pigments, without the analysis of reference products.

Lichens are special organisms, most of them resulting from the association of fungi and algae. They are well-known as pioneers of vegetation, colonizing all types of substrates including tree-bark and bare rock. A large variety of pigments are synthesized in micro-quantities by these organisms, especially when they are exposed to sunlight. Conventional structure elucidation methods, such as UV, IR, NMR and mass spectrometry (MS), involve extraction and purification of the compounds, which in turn involves the risk of chemical artifacts and unexpected losses. Additionally, *in-situ* analysis of these natural products is required to verify the location and distribution of the identified pigments on a micrometer scale. This could be helpful in understanding their biological role in nature. An insight into the microdistribution of pigments within a species might help to understand their interception of sunlight and their possible interaction in transfer of energy.

The *in-situ* analysis of organic molecules in a biological sample on a micrometer scale has been a challenge a mass spectrometrist could not dream of some years ago. Laser microprobe mass spectrometry (LMMS) offers the possibility to analyse samples with 1–5 μm spatial resolution.[1] A focused high-power UV laser produces ions which are detected by MS. Depending on the applied laser power density, elemental and structural information on both organic and inorganic constituents become available. UV irradiation allows the selective desorption and ionization (DI) of products with chromophoric groups. This proves to be a major asset for the analysis of selected organic compounds in a complex biological matrix. Indeed, most organic components other than pigments do not have UV absorbing functionalities and hence are not ionized in LMMS.

The first generation of LMMS instruments with time-of-flight (TOF) mass spectrometers has demonstrated the feasibility of local analysis of organic compounds in botanical samples.[2,3] The high transmission of this type of mass analyser implies high sensitivity. However, only the so-called 'prompt' ions, produced within the 15–20 ns laser pulse, are analysed in TOF LMMS.[1] A variety of products with molecular weight (MW) higher than 500 and with polar groups tend to produce ions after the laser pulse. The analysis of such compounds is not feasible by TOF LMMS. Additionally, low mass-resolution and nominal mass accuracy makes analysis of isolated reference products necessary for interpretation of the mass spectra.

To overcome the instrumental problems of TOF LMMS, new microprobes with Fourier transform (FT) MS detection were developed.[4–6] The high mass resolution offers superior identification capabilities. In principle, the additional analysis of reference products might become superfluous. Obviously, it could be anticipated that sensitivity problems in practical FT LMMS analysis might arise in comparison to TOF LMMS, known as the mass analyser with the best transmission, and hence, the best sensitivity possible. Note, however, that FT LMMS as an ion trap permits the detection of the sum of prompt and post-laser generated ions. One of the questions to be addressed concerns whether or not FT LMMS can handle similar applications to those of TOF LMMS.

This paper describes a study of representative test cases illustrating the *in-situ* application of FT LMMS. In several species, pigments classified as xanthones, anthraquinones, naphthoquinones and pulvinic acid derivatives were studied. Three test cases had already been studied by TOF LMMS.[2] FT LMMS results were aimed at the assessment of the relative sensitivity as well as the gain in specificity and accuracy. The other species will show that the application area in FT LMMS can be extended to a larger group of compounds. Finally, this study will demonstrate that FT LMMS permits the localization of the pigments on a 5 μm scale and at the same time eliminates the need for prior MS investigation of reference products. However, background information from IR and NMR spectrometry is still necessary to fully identify their chemical structure.

EXPERIMENTAL

Analyses were performed on a Spectrospin CMS 47X converted into a laser microprobe (Bruker Instruments, Inc., Billerica, MA, USA) and equipped with an Infinity Cell™[8] in a 4.7 tesla magnet. Ions are generated in the external ion source and transported to the cell by an electrostatic transfer line.[9] Samples are ionized with a frequency-quadrupled Nd:YAG laser, delivering 25 mJ in 10 ns pulses at 266 nm. An optical interface allows the laser beam to be focused down to 5 μm and the laser power density on the sample to be adjusted between 10^7 and 10^{10} Wcm^{-2}. The specimen is irradiated in reflection mode under 45°. The sample can be

† Presented at the 3rd European Workshop on ICR, 4–6 September 1995, Bremen, Germany

* Author for correspondence.

CCC 0951–4198/96/050562–11

Received 28 October 1995
Accepted (revised) 29 January 1996

observed with a low magnification binocular microscope and with an additional 700× microscope, coupled to a charged coupled device (CCD) camera with monitor. Samples collected from nature are cut to such a size so that they can be mounted on the sample holder (20×20×10 mm) by means of double-sided tape. Additional technical information is available elsewhere.[6]

In FT LMMS with an external ion source, mass spectra of low and high m/z ions have to be recorded in distinct steps. Since ions of different m/z, produced simultaneously in the source, have different flight times from source to cell, a time dispersion occurs. Low m/z ions arrive first at the cell, the heavier ones later on. Assuming that all ions are formed at the same moment, ions with different m/z can be trapped and measured together on the condition that the high to low m/z ratio does not exceed a factor of about 2.5 decade. The parameter T_{gate} essentially selects the observation window along the m/z scale. Note that post-laser DI makes that low m/z ions can arrive at the cell together with heavier ones, generated promptly. As a result, FT LMMS always detects the combined contribution of prompt and post-laser desorbed ions over a limited period (50–300 μs) after the laser pulse. An extensive discussion is given elsewhere.[10]

Specimens studied

Laurera sanguinaria Malme: Brazil, 43 km from Guiratinga and 66 km from Rondonopolis, near the bridge across the 'Corrego Taruma', *leg.* A. Mathey and D. Vital; *det.* A. Mathey.

Laurera purpurina (Nyl.) A. Zahlbr.: Cameroun, RN2, 27 km from Bassa, 18 km from Douala, on trees along Road nr. 103, *leg.* et *det.* A. Mathey.

Haematomma ventosum (L.) Mass.: Sweden, Lapland, Björkliden, *leg.* et *det.* A. Mathey

Chiodecton sanguineum Wainio: U.S.A., University of Florida, *leg.* et *det.* A. Mathey

Acarospora hilaris (Duf.) Hue: Italy, South-Sardinia, Baia di Chia, close to the large beach 'La grande spiagia'

Lecanora epanora Ach. *em.* Poelt: United Kingdom, Anglesey, Parys Mountain Copper Mine, V.C. 52, 23/441899, *leg.* et *det.* O.W. Purvis

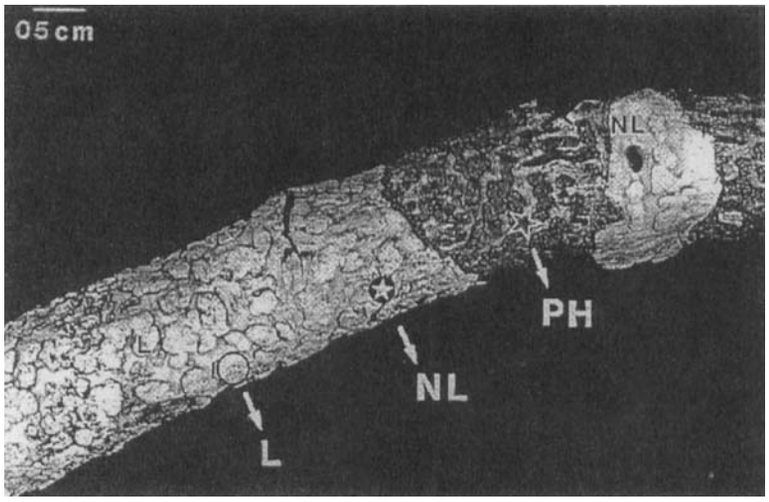

Figure 1. Optical micrograph of a branch covered by two forms of *Laurera sanguinaria*: the form with the superficial orange pigment physcion (PH) covering the warts and the *forma morbosa* with the pale pigment lichexanthone (L) on the warts. The superficial pale thallus pigment is characterised as norlichexanthone (NL) in both forms.

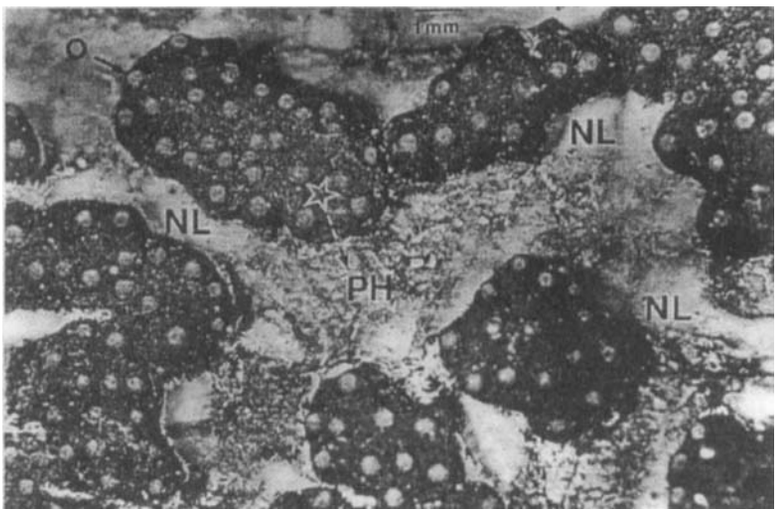

Figure 2. Optical micrograph of the orange form of *Laurera sanguinaria* with physcion (PH) on the warts and the pale thallus pigment, norlichexanthone (NL). The ostioles (O) are the openings exposing the perithecia or fruiting-bodies immersed into the orange warts.

RESULTS AND DISCUSSION

Xanthones and anthraquinones

Two species of the Trypetheliaceae family were chosen to compare the performances of TOF and FT LMMS instruments used for characterizing different types of xanthones and anthraquinones. The Trypetheliaceae family is pantropical and is characterized by the presence of warts. The flask-shaped fruiting bodies (perithecia) are contained by the warts. The openings (ostioles) leave the perithecia exposed.

Laurera sanguinaria is an interesting lichen species found only in Brazil, covering high sun-exposed branches of very tall trees along rivers and is illustrated in Figs. 1 and 2.[11] This species is abundant in Mato Grosso and synthesizes a large variety of pigments, which were extracted and identified, after isolation, by UV, NMR, IR and electron ionization (EI) MS with direct probe introduction.[12] The upper surface of the warts is generally orange coloured. The orange colour can be masked by the formation of a black layer, which may be due to the formation of polymers. A pale form was described as *Laurera sanguinaria* forma *morbosa*.[13] In this study, only the superficial pigments were analysed: the upper pale pigment of the vegetative part (thallus), the pale pigment covering the forma *morbosa* warts and the orange pigment on the warts.

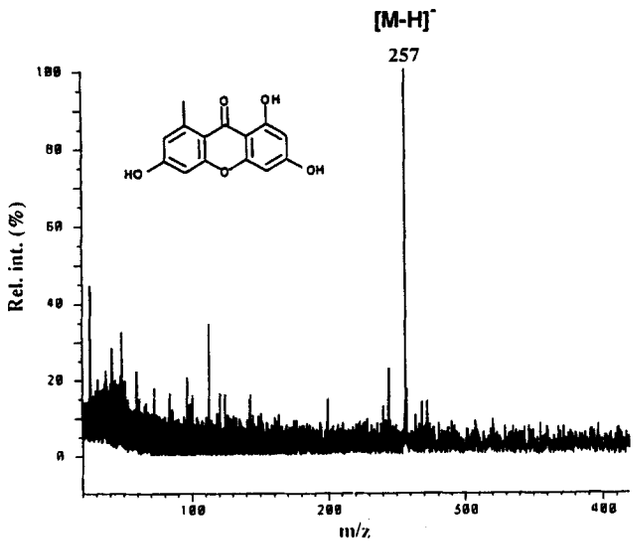

Figure 3. Negative-ion mass spectrum of norlichexanthone recorded from *Laurera sanguinaria* thallus with a power density of 1×10^{10} Wcm^{-2} and a T_{gate} of 400 μs.

Table 1. Mass measurement of diagnostic ions from *Laurera sanguinaria* and *Laurera purpurina*

Measured *m/z*	Elemental composition	Accuracy of mass measurement (ppm)
Norlichexanthone, $C_{14}H_{10}O_5$, MW 258		
negative ions		
257.046	$C_{14}H_9O_5$	0.37
Lichexanthone, $C_{16}H_{14}O_5$, MW 286		
negative ions		
271.061	$C_{15}H_{11}O_5$	0.64
257.046	$C_{14}H_9O_5$	1.80
256.038	$C_{14}H_8O_5$	1.20
241.051	$C_{14}H_9O_4$	0.29
Physcion, $C_{16}H_{12}O_5$, MW 284		
negative ions		
269.046	$C_{15}H_9O_5$	0.41
241.051	$C_{14}H_9O_4$	0.88
240.043	$C_{14}H_8O_4$	0.72
225.056	$C_{14}H_9O_3$	0.52
Xanthorin, $C_{16}H_{12}O_6$, MW 300		
positive ions		
339.027	$C_{16}H_{12}O_6.K$	0.96
negative ions		
285.040	$C_{15}H_9O_6$	0.96
271.025	$C_{14}H_7O_6$	0.51
269.045	$C_{15}H_9O_5$	0.97
257.045	$C_{14}H_9O_5$	1.60

The negative-ion mass spectrum, illustrated in Fig. 3, is obtained from the pale thallus pigment, described before as norlichexanthone (MW 258) using conventional non *in-situ* methods.[14–16] TOF LMMS on a similar sample confirmed the assignment.[2] The base peak in the FT LMMS negative-ion mode results lies at *m/z* 257 and corresponds to the deprotonated molecule of norlichexanthone, as can be confirmed from the high resolution measurement in Table 1. At a shorter T_{gate} in FT LMMS, carbon clusters are detected. As a result, the mass spectral information corresponds to that obtained in TOF LMMS, i.e. carbon cluster and $[M-H]^-$ ions. It should be stressed that also in FT LMMS,

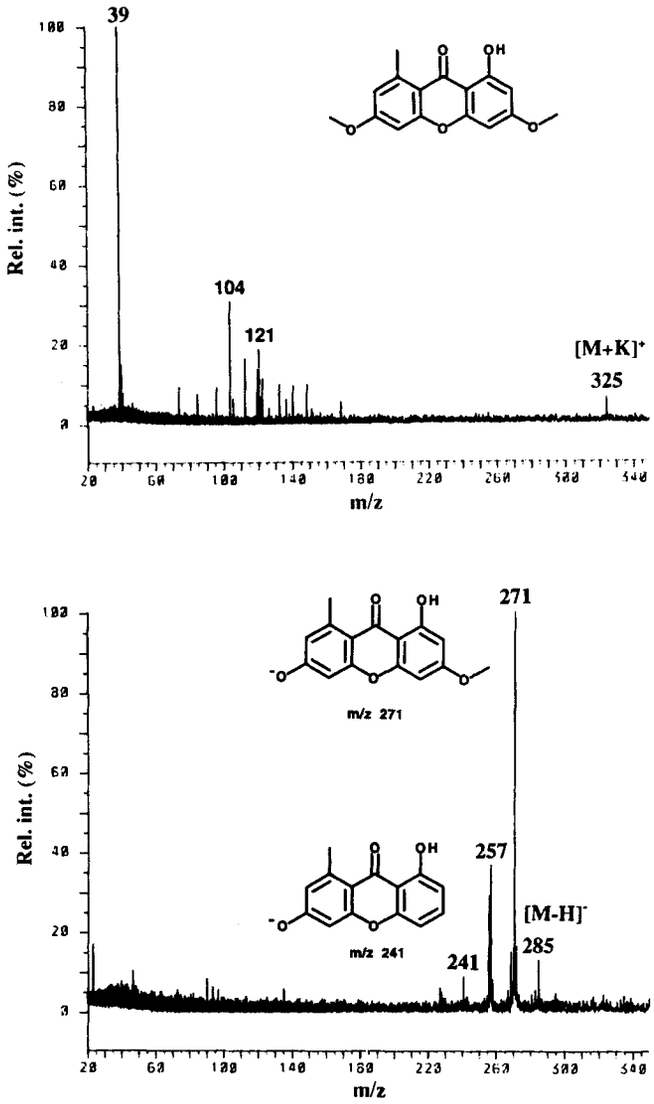

Figure 4. Positive- (top) and negative-ion (bottom) mass spectra of lichexanthone recorded from *Laurera sanguinaria* forma *morbosa* warts with a power density of 1×10^{10} Wcm^{-2} and a T_{gate} of 600 μs and 500 μs, respectively.

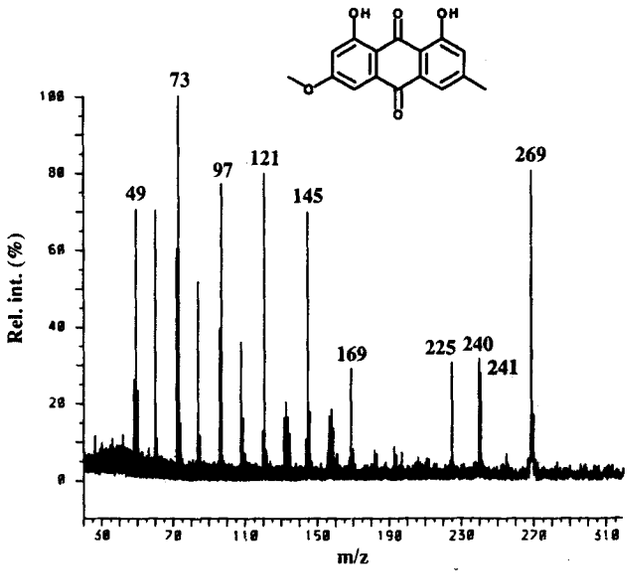

Figure 5. Negative-ion mass spectrum of physcion recorded from *Laurera sanguinaria* orange warts with a power density of 6.8×10^9 Wcm^{-2} and a T_{gate} of 400 μs.

background information is needed from other techniques to give some ideas about the possible structure of the pigment. It would have been impossible to characterize this substance *in-situ*, by the detection of a single fragment ion.

Figure 4 shows the positive- and negative-ion mass spectra from the pale pigment, lichexanthone (MW 286),[15-16] characterizing *Laurera sanguinaria* forma *morbosa*. Compared to TOF LMMS, no structural fragments are detected in the positive-ion mode; only some C_nH_m cluster ions appear in the low *m/z* range, while $[M+K]^+$ ions at *m/z* 325 are observed in FT LMMS, instead of protonated molecules as in TOF LMMS. The reason for the former observation is not yet clear. As to the latter, the local distribution of potassium ions in biological species is heterogeneous and may vary from one sample to another. Hence, since different samples of the same species were analysed, the local potassium concentration could be different. Secondly, according to our tentative DI model, cationization is believed to continue for several microseconds after the laser pulse.[1] Since FT LMMS measures ions formed up to microseconds after the laser pulse, the mass spectra include the sum of prompt and post-laser generated ions. Hence, it is likely that more $[M+K]^+$ ions are sampled by FT LMMS compared with TOF LMMS. Additionally, no structural positively-charged fragments are detected. This is consistent with the hypothesis that the cationized molecules usually issue from ion–molecule reactions in the selvedge and hence do not act as the main precursors of the fragments in LMMS.[1]

As to the negative-ion mode, only fragment ions are detected. The base peak at *m/z* 271 is assigned to the loss of a methyl group, while the $[M-H]^-$ as well as some other fragments are detected. The formal loss of formaldehyde from $[M-CH_3]^-$ results in the ion at *m/z* 241, while the ions at *m/z* 257 and 256 might issue from another molecule. This is supported by the high-resolution measurements in Table 1. Indeed, it is not obvious that lichexanthone would lose respectively an ethyl group or an ethane molecule. This would involve an unlikely skeletal rearrangement. The signals could easily issue from a methyl ether ether from a related pigment with still unknown structure. As to the analysed pigments, the signal at *m/z* 257 could originate from the presence of norlichexanthone (*v. supra*), but then the peak at *m/z* 256 must still correspond to a third component. Xanthorin, located in another species, *Laurera purpurina* (*v. infra*), generates signals at *m/z* 257 and 256, but a more intense peak at *m/z* 285 would also be expected, which is absent in the spectrum of Fig. 4.

The negative ion FT LMMS data on the orange pigment, physcion (MW 284), are shown in Fig. 5 and consist of structural ions at *m/z* higher than 200 and primarily C_nH^- clusters (n=4–14) in the low *m/z* range. The ions at *m/z* 240 are radical and may be formed by the combined loss of $CH_3^{\bullet}$ and $HCO^{\bullet}$ from $M^{-\bullet}$, as can be deduced from the high mass resolution data in Table 1. These ions were also detected by TOF LMMS analysis of the isolated product. This supports

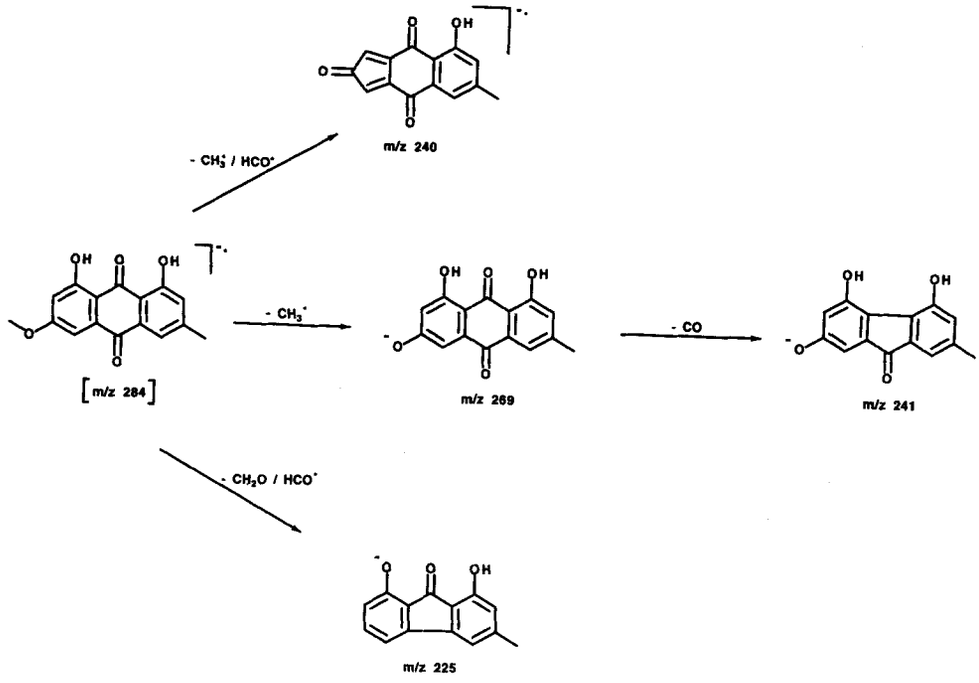

Scheme 1. Tentative fragmentation routes for the orange pigment physcion from *Laurera sanguinaria*.

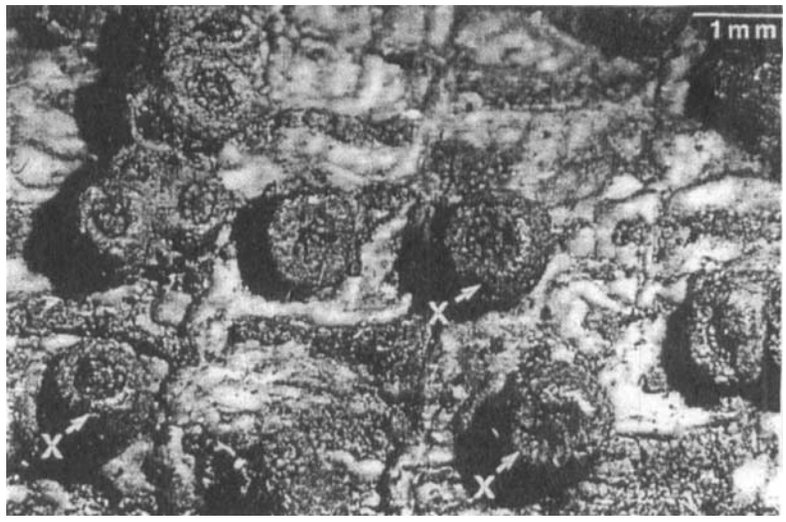

Figure 6. Optical micrograph of *Laurera purpurina* isolated red warts, covered with xanthorin (X).

the assignment of the *m/z* 240 ions as originating from the red pigmented analyte and not from another component in the biological sample. The radical molecular ions are not detected directly, but the occurrence of electron capture ionization (ECI) can be assumed. Hence, the formation of the ions at *m/z* 269 and 241 can be readily explained by cleavage of a methyl radical from the $M^{-\bullet}$ ions, followed by the loss of CO, as shown in Scheme 1. Ions which are not detected in FT LMMS are between brackets. The successive loss of HCO$^{\bullet}$ and formaldehyde from $M^{-\bullet}$ results in the ions at *m/z* 225.

The detection of the radicals at *m/z* 240 in TOF LMMS suggests that these ions are promptly formed and also confirms that in FT LMMS the sum of both prompt and post-laser generated ions is sampled. However, since the residence time of the ions in the external ion source is in the order of microseconds, it is not possible to distinguish whether ECI or dissociative ECI processes are involved. The detection of radical fragments in some of the samples analysed in this study may justify the idea that the formation of the negative ions is explained starting from the molecular ion $M^{-\bullet}$. This is consistent with our DI-model, tentatively proposed on the basis of TOF LMMS results.[1]

Inside the warts of *Laurera sanguinaria*, a new perylenequinone from lichens, isohypocrelline, has already been characterized by FT LMMS.[7]

Laurera purpurina is a pantropical species and can be easily recognized by its red coloured warts. The colour is reported to be due to the anthraquinone xanthorin (MW 300).[17] The analysed species is illustrated in Fig. 6. TOF LMMS has been performed on the isolated compound. In the positive-ion mode, protonated molecules and a small

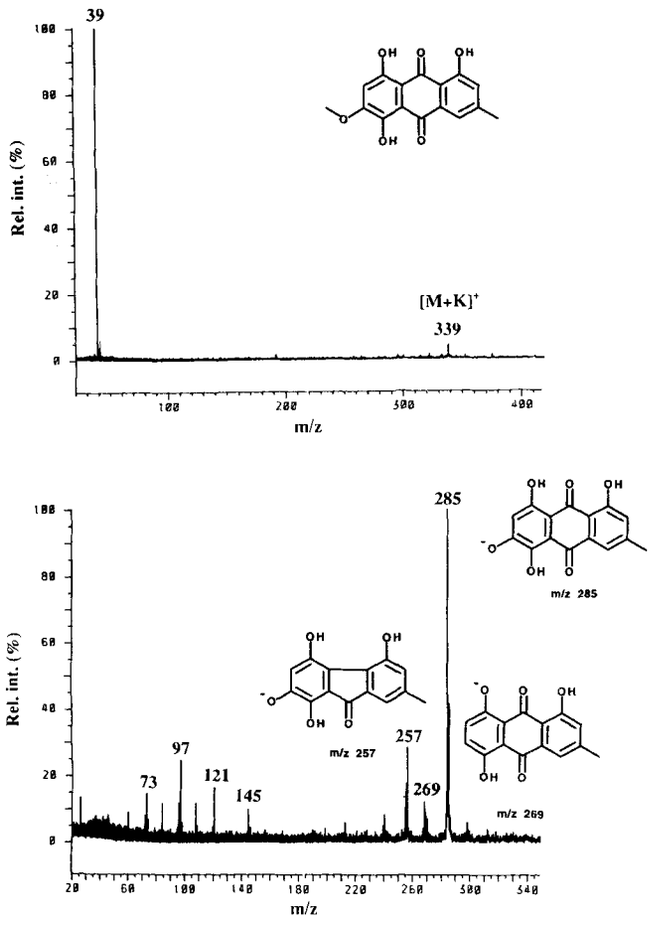

Figure 7. Positive- (top) and negative-ion (bottom) mass spectra of xanthorin recorded from *Laurera purpurina* with both a power density of 6.8×10^9 Wcm^{-2} and a T_{gate} of 500 μs.

Table 2. Mass measurement of diagnostic ions from *Chiodecton sanguineum*

measured *m/z*	elemental composition	accuracy of mass measurement (ppm)
Chiodectonic acid, $C_{15}H_{10}O_9$, MW 334		
positive ions		
372.996	$C_{15}H_{10}O_9 \cdot K$	0.74
negative ions		
333.025	$C_{15}H_9O_9$	0.44
319.010	$C_{14}H_7O_9$	1.75
318.002	$C_{14}H_6O_9$	1.61
291.015	$C_{13}H_7O_8$	0.12
290.007	$C_{13}H_6O_8$	0.90
289.999	$C_{13}H_5O_8$	0.56
275.020	$C_{13}H_7O_7$	0.54
261.004	$C_{12}H_5O_7$	1.21
234.989	$C_{10}H_3O_7$	0.40
221.009	$C_{10}H_5O_6$	0.05
206.994	$C_9H_3O_6$	0.53
206.022	$C_{10}H_6O_5$	1.27
205.014	$C_{10}H_5O_5$	0.04

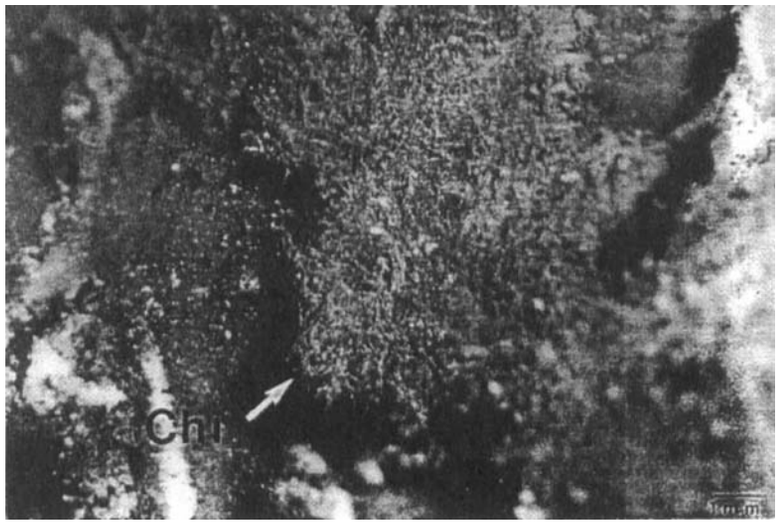

Figure 8. Optical micrograph of *Chiodecton sanguineum* thallus. Red grannular pigments are identified as chiodectonic acid (Chi).

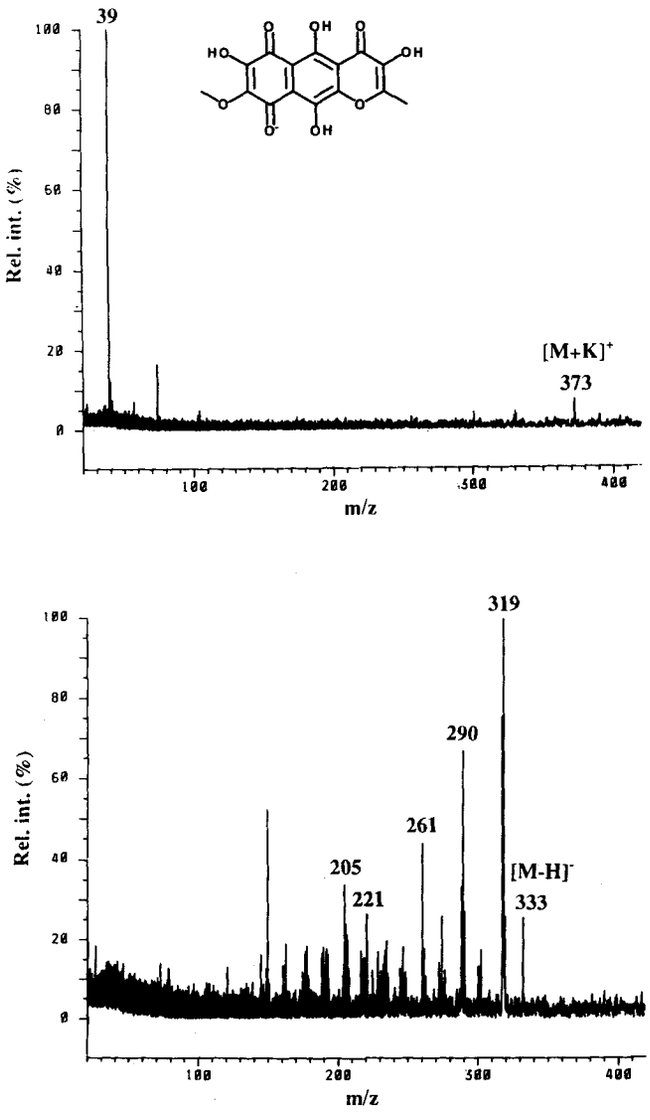

Figure 9. Positive- (top) and negative-ion (bottom) mass spectra recorded from *Chiodecton sanguineum* with a power density of 1×10^{10} Wcm^{-2} and 6.8×10^{9} Wcm^{-2} and a T_{gate} of 600 μs and 400 μs, respectively.

signal from $M^{+\bullet}$ ions were detected as well as two fragment ions at *m/z* 287 and 258. As to the negative ions, a minor $[M-H]^-$ signal at *m/z* 299 and 2 major fragments at *m/z* 285 and 256 occur. Figure 7 shows that all the required information for pigment characterisation is available in FT LMMS from the combination of positive- and negative-ion mass spectra. The MW can be deduced from the K-cationized molecule at *m/z* 339 in the positive-ion mode. No $M^{+\bullet}$ ions were detected. The reason might be that these ions are exclusively promptly formed and hence form only a negligible contribution to the ions detected in FT LMMS. The base peak at *m/z* 285 in the negative-ion mass spectrum is assigned to the $[M-CH_3]^-$ ions, just as in the case of physcion. Other structural fragments can be explained as before, except that at *m/z* 271, which again formally results from the loss of an ethyl group. For the same reasons as stated before, these ions probably originate from another

Table 3. Mass measurement of diagnostic ions from *Haematomma ventosum*

measured *m/z*	elemental composition	accuracy of mass measurement (ppm)
Haemoventosin, $C_{15}H_{12}O_7$, MW 304		
positive ions		
343.022	$C_{15}H_{12}O_7.K$	1.38
negative ions		
305.030	$C_{14}H_9O_8$	0.42
304.059	$C_{15}H_{12}O_7$	0.07
289.035	$C_{14}H_9O_7$	0.41
261.041	$C_{13}H_9O_6$	0.54
261.004	$C_{12}H_5O_7$	1.00
259.061	$C_{14}H_{11}O_5$	0.51
259.025	$C_{13}H_7O_6$	0.65
245.046	$C_{13}H_9O_5$	0.08
245.010	$C_{12}H_5O_6$	1.22
243.030	$C_{13}H_7O_5$	0.87
231.067	$C_{13}H_{11}O_4$	1.12
231.030	$C_{12}H_7O_5$	1.72
230.994	$C_{11}H_3O_6$	0.19
227.035	$C_{13}H_7O_4$	0.06
217.051	$C_{12}H_9O_4$	0.21
217.014	$C_{11}H_5O_5$	0.68
189.020	$C_{10}H_5O_4$	1.10

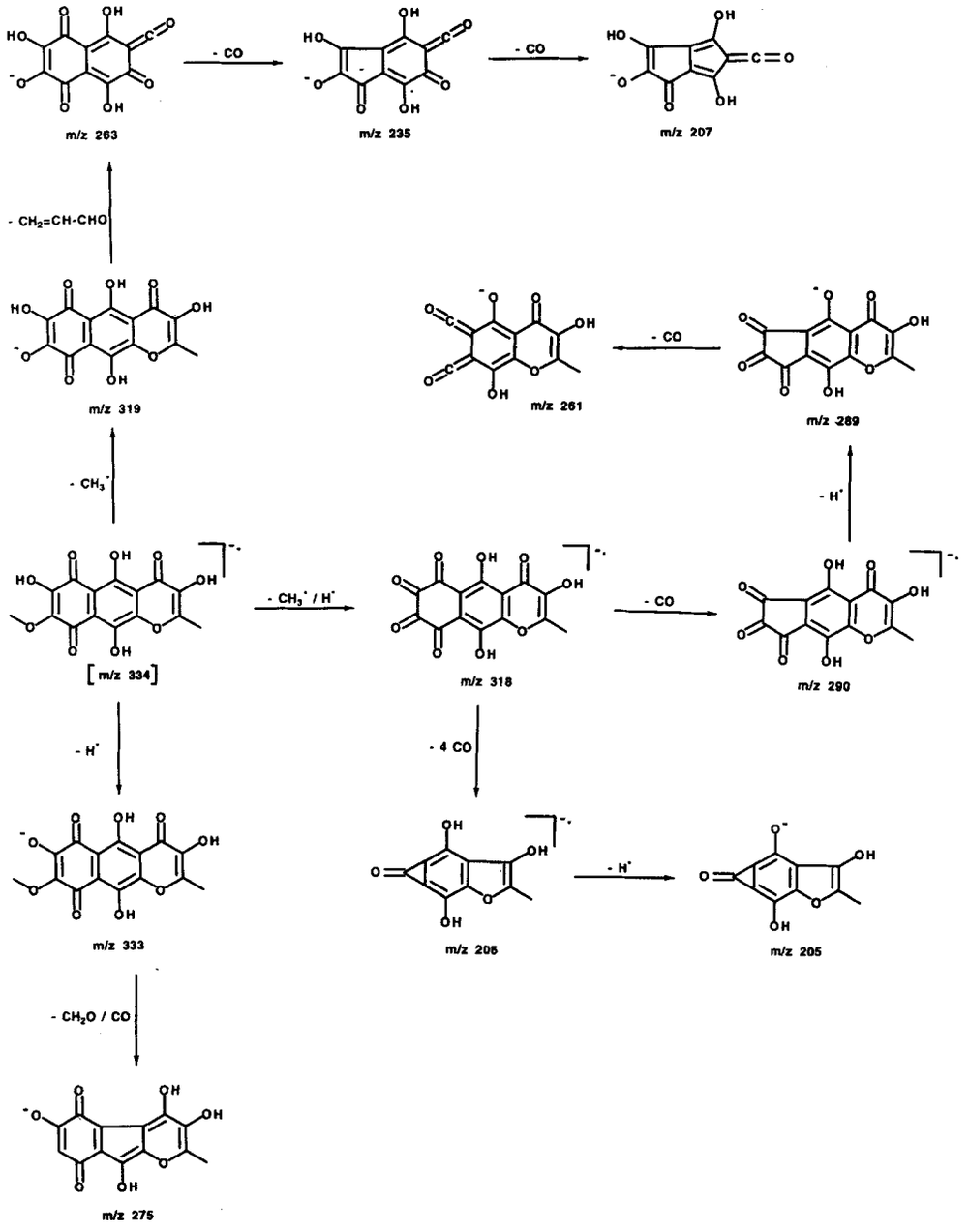

Scheme 2. Tentative fragmentation routes for the pigment chiodectonic acid from *Chiodecton sanguineum*.

molecule. The signals at lower *m/z* are assigned to C_nH^- clusters (n=5–12).

In conclusion, from the species analysed, it has been shown that in those cases where MW information is provided by FT LMMS, it is available as cationized molecules and not as $[M+H]^+$ ions as in TOF LMMS. In the negative-ion mode, more fragment ions are produced, which may be due to the longer residence time the ions spend in the external ion source of the FT LMMS instrument.

Table 4. Mass measurement of diagnostic ions from *Acarospora hilaris* and *Lecanora epanora*

measured *m/z*	elemental composition	accuracy of mass measurement (ppm)
Rhizocarpic acid, $C_{28}H_{23}NO_6$, MW 469		
positive ions		
508.116	$C_{28}H_{23}NO_6.K$	0.35
340.997	$C_{17}H_{11}O_3K.K$	0.76
Epanorine, $C_{25}H_{25}NO_6$, MW 435		
positive ions		
474.132	$C_{25}H_{25}NO_6.K$	0.88
212.842	$K_2SO_4.K$	0.04

Naphthoquinones

Chiodecton sanguineum is widely spread on tree barks in Florida. Its thallus consists of intricate red filaments. The red granular pigments were analysed on the hyphae, consisting of files of cells. Figure 8 illustrates the analysed species. The structure of the isolated pigment (MW 334) had already been determined by conventional methods.[18] In FT LMMS, the MW is available from the potassium cationized ions at *m/z* 373 in the positive-ion mass spectrum in Fig. 9. The extensive set of fragments in the negative-ion mode affords full diagnostic information. The fragmentation routes represented in Scheme 2 are based on the high-resolution mass measurements in Table 2. The pathways are

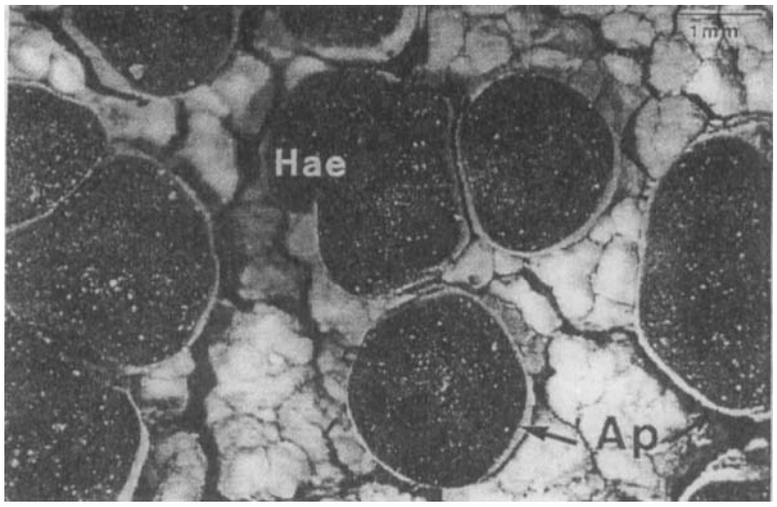

Figure 10. Optical micrograph of *Haematomma ventosum* dark red apothecia (Ap), showing the location of haemoventosin (Hae).

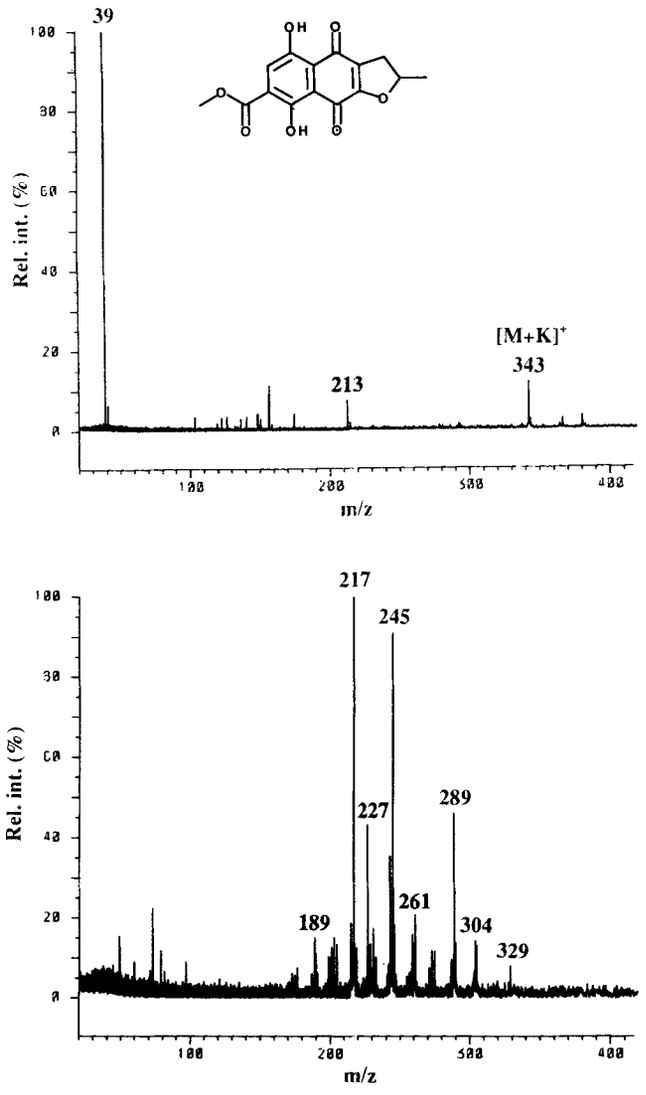

Figure 11. Positive- (top) and negative-ion (bottom) mass spectra recorded from *Haematomma ventosum* with a power density of 1×10^{10} Wcm^{-2} and 5.1×10^{9} Wcm^{-2} and a T_{gate} of 500 μs and 400 μs, respectively.

tentative and no collision-induced dissociation (CID) experiments were attempted. It is believed that the input of extra energy by collisions is not comparable to the process observed in laser microbeam ionization. Hence, CID does not serve to elucidate the fragmentation mechanisms induced by laser DI. The proposed H-transfer between a hydroxyl- and carbonyl group in Scheme 2 can be readily conceived. The ion at *m/z* 275 is derived from the successive loss of formaldehyde and CO from the $[M-H]^-$ ion. Application of well-known rearrangement mechanisms to the $[M-CH_3]^-$ ion at *m/z* 319 can result in an *m/z* 263 ion, which may then lead to the ions at *m/z* 235 and 207 by the subsequent loss of two CO molecules. Three radical fragments are detected at *m/z* 318, 290 and 206 whose formation is easily rationalized by losses of hydrogen and methyl radicals, followed by the expulsion of CO. The remaining fragment ions can be explained by the routes from the ions at *m/z* 290 or 206.

Haematomma ventosum is a saxicolous species, common in Lapland, showing dark red disk-like fruiting bodies, called apothecia, and a yellow thallus. Figure 10 illustrates the analysed species. Only the apothecia were analysed. The structure of haemoventosin (MW 304) had already been determined by conventional methods.[19,20] The positive- and negative-ion mass spectra are shown in Fig. 11, while the high resolution mass measurements are summarized in Table 3. The positive ion at *m/z* 343 is assigned to the potassium cationized molecule. As for the negative ions, molecular ions at *m/z* 304, as well as an extensive set of fragments are detected. Tentative fragmentation routes are presented in Scheme 3. The formation of the fragment ions is again rationalized starting from the molecular anions. Almost all ions can be explained by normal mechanisms, such as loss of CO, formaldehyde, H_2, CO_2 or ethene. Only the ions at *m/z* 259, 231 and 227 involve a rather uncommon methyl transfer or originate from another constituent. The ions at *m/z* 329 and 305 remain unexplained. Comparing the compositions of the ions at *m/z* 305 and 304 in Table 3, it becomes obvious that the former ions result from a different component in the complex biological matrix. It could also be that the ions at *m/z* 304 issue from the fragmentation of another molecule.

In conclusion, these last two examples demonstrate that FT LMMS yields enough information to allow, in combination with IR and NMR results, the characterization of the analysed molecule. The comparative analysis of reference products is not strictly needed but some initial ideas about the possible structure remain mandatory. Also, the presence of several radical negative fragments, and sometimes even $M^{-\bullet}$, clearly points to the fact that ECI occurs in laser microbeam DI, in contrast to common notions about DI in LMMS.[21–24]

Pulvinic acid derivatives

Acarospora hilaris, illustrated in Fig. 12, is characterized by bright yellow patches colonizing bare silicate rocks. The yellow colour is essentially due to rhizocarpic acid

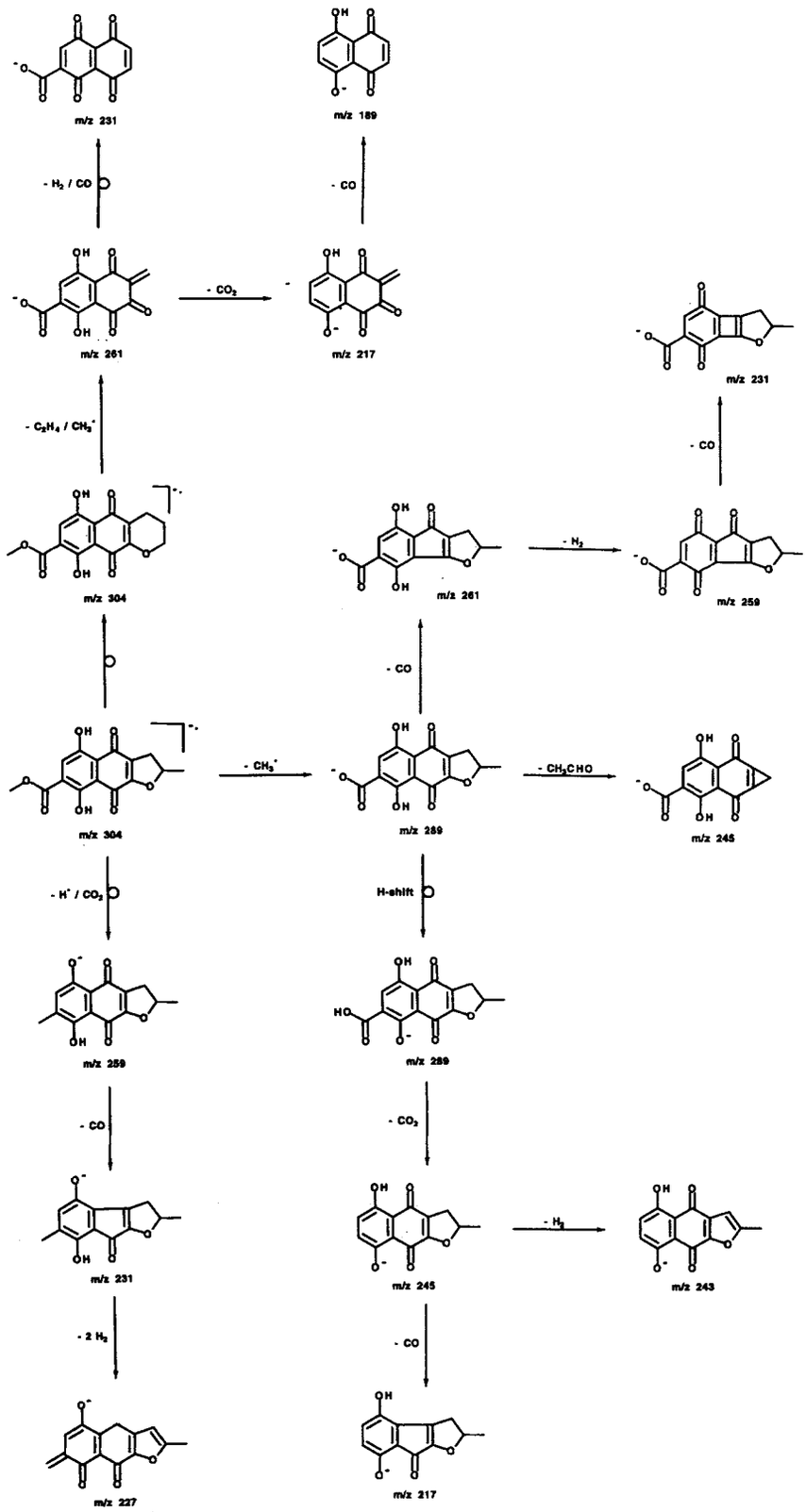

Scheme 3. Tentative fragmentation routes for the pigment haemoventosin from *Haematomma ventosum*.

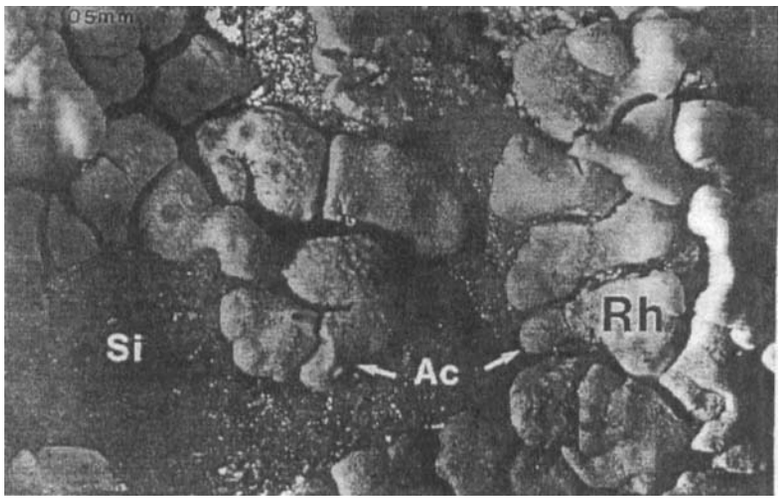

Figure 12. Optical micrograph of *Acarospora hilaris* (Ac) colonizing silica rocks (Si). Rhizocarpic acid (Rh) is located on yellow thallus patches.

(MW 469).[25] Analysis by cathodoluminescence was published elsewhere.[26] This technique permits the precise localization of the pigment by means of the detection of light, emitted under electron bombardment of the sample. The structure specificity of these signals however is not obvious and cannot compete with conventional MS information.

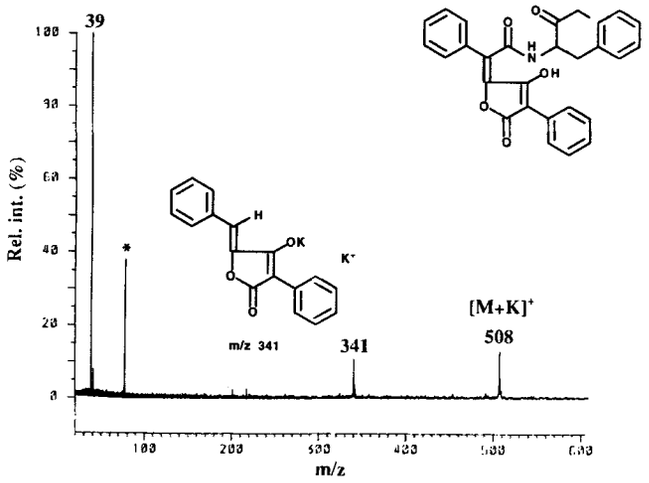

Figure 13. Positive-ion mass spectrum recorded from *Acarospora hilaris* with a power density of 1×10^{10} Wcm^{-2} and a T_{gate} of 600 μs.

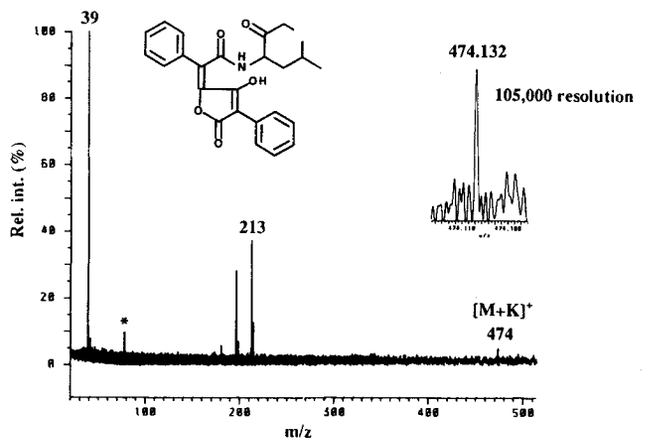

Figure 14. Positive-ion mass spectrum recorded from *Lecanora epanora* with a power density of 1×10^{10} Wcm^{-2} and a T_{gate} of 600 μs.

Figure 13 shows the detection of the potassium cationized molecule at *m/z* 508, and a fragment at *m/z* 341 in the positive-ion mode. High-resolution mass measurements are summarized in Table 4. The fragment ion is formed by the cleavage of the amino-acid moiety and the exchange of an acidic hydrogen by potassium. It is not known whether this fragmentation occurs *in-situ* or during the DI-process in LMMS. The sensitivity for the structural ions is not very high compared to the K^+ ions. However, due to the high mass-resolution and accurate *m/z* determination available in FT LMMS, the specificity is increased compared with TOF LMMS. No negative ions could be detected from this sample. It should be noted that the analysis of molecules with MW higher than 500 would not have been feasible with TOF LMMS. Higher-mass compounds typically produce ions which are formed delayed with respect to the laser pulse. Since TOF LMMS exclusively samples the ions formed within about 15 ns, collection of post-laser generated ions gives rise to an increased background. This leads to peak broadening with incorrect mass calibration and loss of resolution.

Lecanora epanora was chosen as a next test sample because the thallus is reported to contain epanorin, a pigment with similar chemical structure to rhizocarpic acid. This species also colonizes rocks. Figure 14 illustrates the positive FT LMMS mass spectrum with a signal at *m/z* 474 corresponding to the K-cationized molecule. No relevant structural fragment was detected unlike rhizocarpic acid. However, potassium sulphate, probably present in the biological matrix, becomes cationized resulting in the signal at *m/z* 213, which might indicate that the soft ionization process of potassium attachment also extends to inorganic substances. More information about the DI of inorganic compounds can be found elsewhere in this issue.[27]

Note that all the mass spectra have been recorded by the accumulation of more than 100 laser shots, as opposed to TOF LMMS where a full mass spectrum is obtained from each single laser shot. This might reduce the spatial resolution in FT LMMS, unless individual shots are taken from selected spots. Consequently, single shot experiments have to be performed by monitoring a single *m/z* value. This is feasible in the high resolution mode, as illustrated by the inset in Fig. 14, showing a typical high mass-resolution signal from the *m/z* 474 ion. Note that a mass resolution of 100 000 can be routinely obtained in FT LMMS from a

microscopical sample, which is not at all possible in conventional MS.

CONCLUSION

It has been demonstrated in this study that chemical compounds of three different classes could be analysed *in-situ* in lichens by FT LMMS. Due to the reflection geometry, sample preparation could be kept to an absolute minimum. The panoramic recording of a mass spectrum in FT LMMS needs the accumulation of more than 100 shots, as opposed to TOF LMMS where, in principle, a full mass spectrum is available from each single laser shot. The loss in sensitivity in FT LMMS, compared to TOF LMMS, is compensated for by the high mass-resolution and the more accurate m/z determination, yielding more specific information. It was also shown that the analysis of less volatile molecules with MW higher than 500 is now feasible, as opposed to TOF LMMS. This might be due to the integrated collection of prompt and post-laser generated ions in FT LMMS. The presence of several radical negative fragments and even molecular ions indicates that electron capture ionization or dissociative ECI must be involved in laser microbeam DI. This contradicts the common notions about DI in LMMS. FT LMMS eliminates the formerly required two-step approach of high mass-resolution analysis of the isolated pigment and subsequent local analysis by TOF LMMS with low mass-resolution. Some information about the chemical structure of pigments is, however, still necessary.

Acknowledgments

Wim Van Roy and Luc Van Vaeck are indebted to the National Science Foundation of Belgium (N.F.W.O.) as research assistant and research director respectively. Annick Mathey is very grateful to the Deutsche Forschungsgemeinschaft. The authors thank Dr. D. Vital and the Institute of Botany of Saô Paulo, Prof. W. Steglich (Univ. of Munich) for the gift of xanthorin, Dr. G. Eckhardt (Univ. of Bonn) for EI spectra, Dr. W. Purvis (Natural History Museum, London) for providing *Lecanora epanora* and Irène Gaspard for printing the photographs.

REFERENCES

1. L. Van Vaeck, H. Struyf, W. Van Roy and F. Adams, *Mass Spectrom. Rev.* **13**, 189 and 209 (1994).
2. A. Mathey, L. Van Vaeck and W. Steglich, *Anal. Chim. Acta*, **195**, 89 (1987).
3. A. Mathey, L. Van Vaeck and P. Ricci, *Microbeam Analysis-1989*, ed. P. E. Russell, p. 350, San Francisco Press, San Francisco, 1989.
4. M. Pelletier, G. Krier, J. F. Muller, D. Weil and M. Johnston, *Rapid Commun. Mass Spectrom.* **2**, 146 (1988).
5. J. T. Brenna, W. R. Creasy, W. McBain and C. Soria, *Rev. Sci. Instrum.* **59**, 873 (1988).
6. L. Van Vaeck, W. Van Roy, H. Struyf, F. Adams and P. Caravatti, *Rapid Commun. Mass Spectrom.* **7**, 323 (1993).
7. A. Mathey, W. Van Roy, L. Van Vaeck, G. Eckhardt and W. Steglich, *Rapid Commun. Mass Spectrom.*, **8**, 46 (1994).
8. P. Caravatti and M. Alleman, *Org. Mass Spectrom.*, **26**, 514 (1991).
9. P. Grossmann, P. Caravatti, M. Alleman and H. Kellerhals, *Proceedings of the 36th ASMS Conference, San Francisco*, ASMS, East Lansing, 1988, pp. 616–617.
10. H. Struyf, W. Van Roy, L. Van Vaeck, R. Van Grieken, R. Gijbels and P. Caravatti, *Anal. Chim. Acta*, **283**, 139 (1993).
11. G.O.A.N. Malme, *Ark. för Botan.*, **19**, 1 (1924).
12. A. Mathey, *De* in-situ *Lichenum investigatione*, Doctorat d'Etat es Sciences Naturelles, Univ. Paris 6, 1987.
13. M. A. Letrouit-Galinou, *Rev. Bryol. Lichénol.*, 207 (1957).
14. D. Broadbent, R. P. Mabelis and H. Spencer, *Phytochem.*, **14**, 2082 (1975).
15. J. Santesson, *Ark. för Kemi*, **30**, 461 (1968).
16. J. Santesson, *Ark. för Kemi*, **30**, 479 (1968).
17. W. Steglich, W. Lösel and W. Reiniger, *Tetrahedron Lett.*, **47**, 4719 (1967).
18. S. Huneck, *Phytochem.*, **15**, 799 (1976).
19. T. Bruun and A. Lamvik, *Acta Chem. Scand.*, **25**, 483 (1971).
20. Y. J. Solberg, *Acta Chem. Scand.*, **1**, 1477 (1957).
21. H. J. Heinen, *Int. J. Mass Spectrom. Ion Phys.*, **39**, 309 (1981).
22. D. M. Hercules, R. J. Day, K. Balasanmugan, T. A. Dang, C. P. Li, *Anal. Chem.*, **54**, 280A (1982).
23. F. P. Novak, K. Balasanmugan, K. Viswanadham, C. D. Parker, Z. A. Wilk, D. Mattern and D. M. Hercules, *Int. J. Mass Spectrom. Ion Phys.*, **53**, 135 (1983).
24. J. Rosmarinowsky, M. Karas and F. Hillenkamp, *Int., J. Mass Spectrom. Ion Phys.*, **67**, 109 (1985).
25. R. M. Letcher and S. H. Eggers, *Tetrahed. Lett.*, **36**, 3541 (1967).
26. A. Mathey, D. Dingley, L. Van Vaeck and R. Young, *Electr. Microsc.*, **3B**, 791 (1994).
27. H. Struyf, L. Van Vaeck and R. Van Grieken, "Desorption-ionisation of inorganic compounds in Fourier transform laser microprobe mass spectrometry with external ion source", *Rapid Commun. Mass Spectrom.*, **10**, (1996).